J. Fluid Mech. (1995), *vol.* 295, *pp.* 229–245

Shear-free turbulent boundary layers. Part 2. New concepts for Reynolds stress transport equation modelling of inhomogeneous flows

By BLAIR PEROT† AND PARVIZ MOIN‡
Department of Mechanical Engineering, Stanford University, Stanford, CA 94305, USA

(Received 10 January 1994 and in revised form 18 February 1995)

Models for the dissipation tensor and (slow) pressure–strain terms of the Reynolds stress transport equations are presented which are applicable near boundaries. These models take into account the large inhomogeneity and anisotropy that can be present near walls and surfaces, and are inspired by the physical insights developed in Part 1 of this paper. The dissipation tensor model represents a fundamentally new approach to dealing with turbulence inhomogeneities. The pressure–strain model shows how the classic return-to-isotropy model of Lumley (1978) can be adapted to the near-wall region. The closure hypotheses underlying these two models are tested in an *a priori* fashion using direct numerical simulation (DNS) data.

1. Introduction

With a few notable exceptions (Durbin 1993; Launder & Shima 1989), the development of Reynolds stress transport equation models has tended to focus on unbounded flows such as shear layers, jets and homogeneous turbulence. In order to apply these models to wall-bounded flows of engineering interest, modifications must be made to account for the near-wall physics. The early works of Launder, Reece & Rodi (1975) and Hanjalic & Launder (1976) discuss 'wall reflection' effects and the 'wall echo' of the pressure. In order to account for these effects, functions of the wall-normal distance (or wall-normal vector) were used to alter the behaviour of various terms in the equations (principally the pressure–strain and dissipation tensor). Similar modifications were made by Gibson & Rodi (1989) to account for the effects of a free surface.

More recently, considerable effort has been devoted to eliminating explicit dependence on the wall-normal coordinate from Reynolds stress transport models. Functions of the stress invariants, and sometimes the Reynolds number, are now generally used (see Tselepidakis 1991 or Hallback 1993). This makes the models applicable in complex domains. There has also been some interest in developing models which have the correct limiting behaviour as the wall is approached (Lai & So 1990; Launder & Reynolds 1983). The present work recognizes the importance of these developments. The models presented herein have the correct limiting behaviour for both walls and free surfaces, they do not include the wall-normal coordinate or the wall-normal vector, and they do not involve functions which must be externally specified.

† Currently at Los Alamos National Laboratory, NM 87545, USA.
‡ Also with NASA-Ames Research Center, Moffet Field, CA 94035, USA.

The turbulence near a wall or surface is strongly inhomogeneous and anisotropic. The assumption of quasi-homogeneity, implicit to most Reynolds stress transport equation modelling, is no longer applicable. We must therefore look directly at the near-wall physics for modelling inspiration. The effects of mean shear produced by a wall are relatively easy to model. It is the more subtle effects of the wall, the 'wall proximity' effect, which is crucial to the development of better near-wall Reynolds stress transport equation models. The shear-free boundary layers analysed in Part 1 (Perot & Moin 1995) provide the physical inspiration for modelling these more subtle effects. The models which are presented herein extend classical quasi-homogeneous models into the near-wall region. Away from the boundary they revert to their classical counterparts. For this reason, it is felt that these models reflect additional physics, not alternative physics, and therefore will be useful in a wide variety of engineering flows.

2. Dissipation model

What is described in this section is not so much a new model, but a technique for extending classical (quasi-homogeneous) models for the dissipation tensor into regions of large inhomogeneity (such as the near-wall region). Unlike previous techniques which were ultimately *ad hoc* in nature, this model for the near-wall dissipation tensor is based on a simple mathematical decomposition and physical observations of the behaviour of near-wall turbulence.

2.1. *Physical inspiration*

The physical inspiration for the dissipation model is found in figure 1. This figure is from simulations of a shear-free solid wall (Part 1). In these simulations a solid no-slip wall is suddenly inserted into isotropic homogeneous decaying turbulence. The wall interacts with the turbulence, creating a boundary layer in the turbulent statistics which grows into the turbulence as time progresses.

The figure shows two planes parallel to the solid wall. The shading indicates the magnitude of the instantaneous tangential velocity. The plane in figure 1 (*a*) is far from the wall, and the min/max values indicate that the r.m.s. intensity is very close to its free-stream value. The plane in figure 1 (*b*) is much closer to the wall and has much smaller min/max levels (and r.m.s. intensities). The crucial observation from these figures is that the structure of the turbulence in two planes is very similar (i.e. the location of the contours), while the magnitude or scale of the turbulent fluctuations (measured either by the min/max of the contours or by the r.m.s. intensities) differs by an order of magnitude from one plane to the other. The distance over which the turbulent intensities are damped by the wall is much smaller than the distance over which the eddy structure (as measured by the eye) changes appreciably. This implies that in very near-wall turbulence, there is a separation of scales, with the turbulent intensities changing much more rapidly than variations in the actual eddy structure. These observations also apply in the near-wall region of the standard flat-plate boundary layer (the shape of the streaks does not change as rapidly as the r.m.s. intensities, as one approaches the wall). Whether these observations apply in even more complicated situations is not a crucial point, since this is the inspiration, not the foundation, for the dissipation tensor model.

The decomposition of turbulence into a generalized turbulent intensity component and a turbulent structure component can be accomplished mathematically in the following way:

$$u_i = \bar{Q}_{ip}\tilde{u}_p. \tag{1}$$

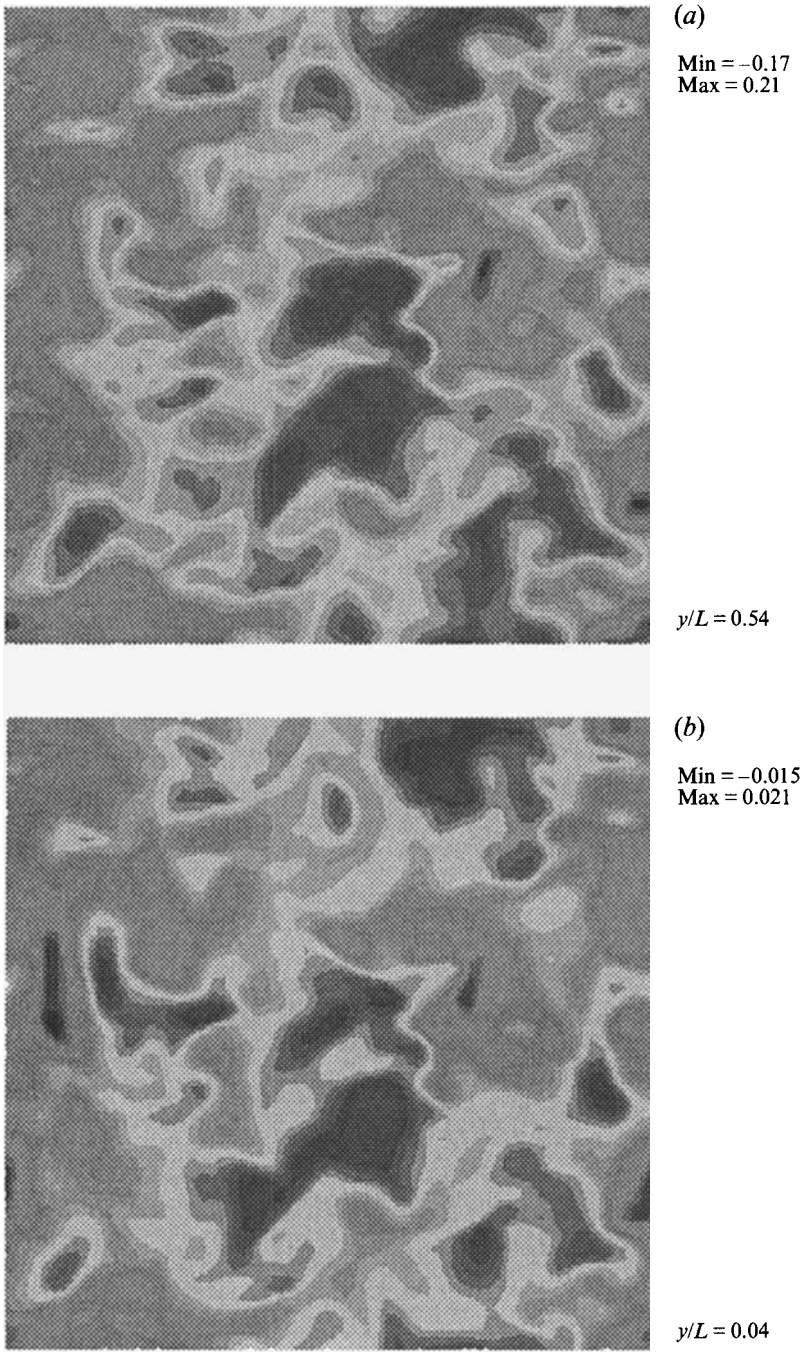

FIGURE 1. Contours of instantaneous tangential velocity in planes parallel to a shear-free solid wall. (Turbulent Reynolds number = 134.)

Here, u_i is the fluctuating velocity (with zero mean), $\bar{Q}_{ip}$ is a generalized turbulent intensity, and $\tilde{u}_p$ is the velocity structure. This operation can also be thought of as a mapping or a transformation which scales the fluctuating velocity component, so that the resultant quantity, $\tilde{u}_p$, is nearly statistically homogeneous. Several appropriate

choices for $\bar{Q}_{ip}$ which accomplish this goal will be discussed in §2.3. However, at this point it is sufficient to observe that (1) is a mathematical decomposition, which is well defined as long as $\bar{Q}_{ip}$ is an invertible matrix.

The turbulent intensity, $\bar{Q}_{ip}$, has an overbar to indicate that it is considered to be a statistical average of turbulence quantities and a known quantity (related in some way to the r.m.s. intensities). Mathematically, the definition of $\bar{Q}_{ip}$ is arbitrary, but physically it is important to choose a definition for $\bar{Q}_{ip}$ which reflects its intended function as a measure of the turbulent intensity. In the context of this work, two definitions for $\bar{Q}_{ip}$ will be considered. One definition is based on the turbulent kinetic energy and the other is based on the Reynolds stress tensor. It is our observation that better definitions for $\bar{Q}_{ip}$ tend to produce better models, at the price of increased model complexity. The choices proposed in this paper are not necessarily optimal.

Having chosen a definition for the generalized turbulent intensity, the properties of the velocity structure can then be derived from (1). The velocity structure (unlike the turbulent intensity tensor) retains the random spatial and temporal fluctuations of the original velocity field. The velocity structure can be thought of as a normalized fluctuating velocity scaled by the generalized turbulent intensity tensor. The result of this normalization by the generalized turbulent intensity is that the velocity structure becomes a homogeneous, or at least a quasi-homogeneous, turbulence quantity. It now becomes possible to think of the decomposition (equation (1)) as a splitting of turbulence into a fluctuating component (the velocity structure) and a generalized intensity (the turbulent intensity tensor).

An analogy with Reynolds decomposition into mean and fluctuating velocities can be made. In the present case, the decomposition is multiplicative rather than additive, and rather than subtracting off the mean to get to fluctuating velocity, we are dividing by some turbulent intensity (the variance) to get the velocity structure. The unknown turbulent quantity of interest (the velocity structure) now has zero mean and unity (or nearly unity, depending on the choice of $\bar{Q}_{ij}$) variance. Like Reynolds decomposition, this is a useful procedure because it extracts, as much as possible, the known statistical properties of the turbulence.

2.2. *Mathematical details*

The result of substituting this mathematical decomposition (equation (1)) into the definition for the homogeneous dissipation tensor,

$$\epsilon_{ij} \equiv 2\nu\overline{u_{i,p}\,u_{j,p}} \tag{2}$$

is

$$\begin{aligned}\epsilon_{ij}/(2\nu) = {} & \bar{Q}_{im,p}\overline{(\tilde{u}_m\tilde{u}_n)}\,\bar{Q}_{jn,p} + \bar{Q}_{im}\overline{(\tilde{u}_{m,p}\tilde{u}_{n,p})}\,\bar{Q}_{jn} \\ & + \tfrac{1}{2}(\bar{Q}_{im,p}\overline{(\tilde{u}_m\tilde{u}_n)}_{,p}\,\bar{Q}_{jn} + \bar{Q}_{im}\overline{(\tilde{u}_m\tilde{u}_n)}_{,p}\,\bar{Q}_{jn,p}) \\ & + \tfrac{1}{2}(\bar{Q}_{im,p}\,W_{mnp}\,\bar{Q}_{jn} - \bar{Q}_{im}\,W_{mnp}\,\bar{Q}_{jn,p}),\end{aligned} \tag{3}$$

where the tensor $W_{mnp} = (\overline{\tilde{u}_m\tilde{u}_{n,p}} - \overline{\tilde{u}_{m,p}\tilde{u}_n})$ is antisymmetric in m and n.

This expression for the dissipation tensor splits the dissipation into three fundamental parts: the dissipation due to spatial variations in the generalized turbulent intensity (first term on the right-hand side), the dissipation due to spatial variations in the turbulent structure (second term on the right-hand side), and coupling terms representing the interaction of the first two dissipation terms with each other (last two terms on the right-hand side).

The contribution to the dissipation due to variations in the generalized turbulent intensity (first term on the right-hand side) dominates in regions of large inhomogeneity where the turbulent intensity changes rapidly. This 'inhomogeneity term' depends

only on the turbulent intensity tensor and the Reynolds stress tensor (by definition, $\overline{\tilde{u}_m \tilde{u}_n} = \bar{Q}^{-1}_{im} R_{ij} \bar{Q}^{-1}_{jn}$ where $R_{ij} = \overline{u_i u_j}$). The generalized turbulent intensity, $\bar{Q}_{ij}$, is assumed to be well defined in terms of other quantities available in the closure, so the inhomogeneity term does not need to be modelled. Because (3) is an exact expression, the inhomogeneity term can also be thought of as an 'exact term'. In regions where the inhomogeneity term dominates (such as near walls), (3) will give exact results for the dissipation tensor.

The second term on the right-hand side of (3) involves a statistical quantity which will be called the structure dissipation tensor. This quantity is much easier to model than the dissipation tensor itself because the velocity structure is, in fact, quasi-homogeneous. Therefore, models based on the assumption of quasi-homogeneity (i.e. most classical dissipation tensor models) can be expected to work very well for this quantity.

The final two coupling terms can be thought of as redistribution terms. The first coupling term (like the first term) does not need to be modelled. The second coupling term must be modelled, but is zero for homogeneous turbulence or when $\bar{Q}_{ij}$ is a diagonal matrix. In the case where $\bar{Q}_{ij}$ is not diagonal, the second coupling term only contributes significantly to the off-diagonal components of the dissipation tensor, and even then it is relatively small.

2.3. *Dissipation model*

There are a number of choices that can be made for the generalized turbulent intensity tensor, $\bar{Q}_{ij}$. A simple choice is an isotropic tensor proportional to the square root of the turbulent kinetic energy, $\bar{Q}_{ij} = k^{1/2}\delta_{ij}$, where k is the turbulent kinetic energy. The resulting expression for the dissipation then becomes

$$\frac{\epsilon_{ij}}{2\nu} = (k^{1/2})_{,p}(k^{1/2})_{,p}\frac{R_{ij}}{k} + \tfrac{1}{2}(k)_{,p}\left(\frac{R_{ij}}{k}\right)_{,p} + k\overline{\tilde{u}_{i,p}\tilde{u}_{j,p}}. \tag{4}$$

This equation is attractive because of its simplicity. The only term requiring modelling is the velocity structure dissipation, $\tilde{\epsilon}_{ij} = 2\nu\overline{\tilde{u}_{i,p}\tilde{u}_{j,p}}$. The inhomogeneity term and redistribution term (the first and second terms on the right-hand side) are well defined, and in the sense described previously, they are 'exact'. Despite its attractiveness, this model suffers from some basic flaws. In particular, it is only weakly realizable: the kinetic energy is guaranteed to remain positive when using this model, but the Reynolds stress tensor itself may become indefinite. Taking the trace of (4) gives the expression $\epsilon = 2\nu(k^{1/2})_{,p}(k^{1/2})_{,p} + k\tilde{\epsilon}$. The quantity $k\tilde{\epsilon}$ can then be recognized as the *modified dissipation* ($\hat{\epsilon}$) suggested by Hanjalic & Launder (1976). This equation provides a mathematical justification for this frequently used quantity.

A better dissipation model can be obtained by using a slightly more complicated choice for the velocity scale tensor, $\bar{Q}_{im}\bar{Q}_{jm} = R_{ij}$. This makes $\bar{Q}_{ij}$ a generalized square root of the Reynolds stress tensor. This square root is not unique. For example, if $\bar{Q}_{im}$ is lower triangular, then $\bar{Q}_{im}$ is the Cholesky decomposition of R_{ij}. If $\bar{Q}_{im}$ is symmetric, then a somewhat more standard tensor square root is obtained, where the eigenvalues of $\bar{Q}_{im}$ are the square roots of the eigenvalues of R_{ij} and the eigenvectors of the two matrices are the same. Because R_{ij} is positive definite, the square root is well defined. The sign of the square root is not important in the model because all terms involving the generalized intensity appear in pairs, cancelling any dependence on the sign. In our limited experience, the actual choice of which square root to use has not been critical: both the Cholesky decomposition and symmetric square root yield very similar results.

The matrix square root is a natural generalization of the definition used to derive (4). Irrespective of the form of $\bar{Q}_{im}$, the relation $\bar{Q}_{im}\bar{Q}_{jm} = R_{ij}$ implies that $\overline{\tilde{u}_i \tilde{u}_j} = \delta_{ij}$, indicating that the velocity structure is nearly homogeneous and isotropic (higher-order moments of $\tilde{u}_i$ cannot be guaranteed to be isotropic, but might be expected to be nearly so). With the generalized intensity tensor defined by $\bar{Q}_{im}\bar{Q}_{jm} = R_{ij}$, the expression for the dissipation takes the form

$$\epsilon_{ij} = 2\nu\bar{Q}_{im,p}\bar{Q}_{jm,p} + \bar{Q}_{im}\tilde{\epsilon}_{mn}\bar{Q}_{jn} + \nu(\bar{Q}_{im,p}W_{mnp}\bar{Q}_{jn} - \bar{Q}_{im}W_{mnp}\bar{Q}_{jn,p}), \quad (5)$$

where $\tilde{\epsilon}_{mn} = 2\nu\overline{\tilde{u}_{m,p}\tilde{u}_{n,p}}$ is, again, the velocity structure dissipation tensor.

The first two terms of (5) are the now familiar inhomogeneous and homogeneous dissipation terms. The inhomogeneous term is 'exact' and the homogeneous term can be modelled with any classical quasi-homogeneous dissipation model. The third term of (5) (the term in parentheses) acts as a redistribution term. It is the second coupling term of (3) (the first coupling term is identically zero). The redistribution term is non-zero only when $\bar{Q}_{im}$ has off-diagonal components, and is identically zero for a shear-free wall and a free surface. It is non-zero in fully developed turbulent channel flow, but contributes only to the off-diagonal dissipation component. Calculations of the redistribution term for an adverse pressure gradient boundary layer (Yang Na 1994, private communication) suggest that even for the off-diagonal dissipation, the redistribution term can be neglected. A probable explanation for the unimportance of the redistribution term is the fact that this term represents a coupling between mechanisms which occur at different scales. As indicated in figure 1, there is a significant difference in the scale over which the inhomogeneity in the turbulence changes and the scale over which the structure of the turbulence changes. In what follows, the redistribution term will be modelled by assuming that it is zero.

2.4. *Mathematical constraints*

It can be shown that every component of this model has the correct leading (and often higher-order) terms in a Taylor series expansion about a no-slip wall or a free surface. This non-trivial result holds irrespective of the model for the structure dissipation as long as the structure dissipation approaches a constant near the wall. It is a result of the fact that inhomogeneity dominates near boundaries, and the inhomogeneous term of (5) is exact.

It is important that models have the correct asymptotic behaviour as they approach the wall (Launder & Reynolds 1983). For instance, at a solid wall the transverse components of the dissipation (ϵ_{11} and ϵ_{33}) must exactly balance the corresponding diffusion components. The boundary conditions imposed at the wall ($\partial R_{11}/\partial y = 0$, $R_{11} = 0$) will force this criterion to be true. If the dissipation is incorrect at the wall, the diffusion (and hence the solution) will also be incorrect at the wall. Some dissipation tensor models (see Lai & So 1990) have the limiting behaviour for a no-slip wall imposed upon them. These models will probably fail when presented with any other type of boundary such as a free surface, a transpiring wall, etc. This is not the case for the current model, which does not impose asymptotic behaviour but which obtains the correct asymptotic behaviour (whenever inhomogeneity dominates) by virtue of the 'exact' inhomogeneous term.

The present model also satisfies certain mathematical constraints. By its construction, the model is Galilean and tensorally invariant. It can be seen from (5) (with $W_{mnp} = 0$) that if the structure dissipation tensor is positive definite, then the dissipation tensor can also be guaranteed to be positive definite. Realizability (Schumann 1977) in the shear-free low Reynolds number limit can be shown by

neglecting all but the viscous terms in the Reynolds stress evolution equations and evaluating the system of equations in the principal coordinate system of the Reynolds stress tensor. If it is assumed that $W_{mnp} = 0$ and $\bar{Q}_{ij}$ is symmetric, then it can be shown (see the Appendix) that

$$\bar{Q}_{\alpha\alpha,t} = \nu \bar{Q}_{\alpha\alpha,kk} - \bar{Q}_{\alpha\alpha}\hat{\epsilon}_{\alpha\alpha}/2, \tag{6}$$

where $\hat{\epsilon}_{\alpha\alpha}$ is the structure dissipation tensor evaluated in the principal coordinate system (like $\bar{Q}_{\alpha\alpha}$ this is a diagonal matrix). Since the eigenvalues of $\bar{Q}_{ij}$ are simply the square roots of the eigenvalues of R_{ij} (by the assumption of symmetry), this equation indicates that non-zero turbulent intensities diffuse and decay exponentially in time, never actually reaching zero. Equation (6) also guarantees that stresses that start at zero (such as at a solid wall) will remain zero for all time. Together, these conditions guarantee that this model will not cause the Reynolds stress tensor to become indefinite as time advances.

2.5. *Results*

The results presented in this section are *a priori* tests of the model. That is to say, DNS data for the Reynolds stresses and dissipation rate, ϵ, are used when evaluating the model. The alternative, solving a closed set of Reynolds stress evolution equations with the model incorporated in the equations, has not been performed. An *a priori* test has been used because it specifically evaluates the closure hypotheses underlying a particular model (our primary concern here). It does not say anything about the solvability of the resultant Reynolds stress transport equation model.

Two classical models for the dissipation tensor assume that dissipation is isotropic ($\epsilon_{ij}^{ISO} = \frac{2}{3}\epsilon\delta_{ij}$) or that the dissipation is proportional to the Reynolds stress tensor (Rotta 1951), ($\epsilon_{ij}^{R} = (\epsilon/k)\,R_{ij}$). A quick look at the DNS results in the following figures indicates that the assumption of isotropy is not a good one near boundaries. We will, therefore, make comparisons only with Rotta's model. The fact that Rotta's model does not obtain the right limit (isotropy) at very high Reynolds numbers led Hanjalic & Launder (1976) to propose a mixed model which uses a Reynolds-number-dependent blending function to obtain the right behaviour at high Reynolds numbers. The functional form of the blending function is found empirically. However, Mansour, Kim & Moin (1988) found that for DNS of turbulent channel flow, this more complicated formulation did not show any improvement over the Rotta model.

In order to test the inhomogeneity model, a model for the structure dissipation tensor,

$$\tilde{\epsilon}_{mn} = 2\nu\overline{\tilde{u}_{m,k}\tilde{u}_{n,k}}, \tag{7}$$

must be assumed. We will assume the simplest possible model for that quantity:

$$\tilde{\epsilon}_{mn} = \tfrac{2}{3}\tilde{\epsilon}\delta_{mn}, \tag{8}$$

where $\tilde{\epsilon}$ is one half of the trace of the structure dissipation tensor. This is essentially the classic isotropy model, but applied to the structure dissipation. Besides its simplicity, this model has some physical justification, since the structure dissipation should be close to homogeneous and isotropic. The near isotropy of the structure dissipation was the very motivation for the velocity decomposition given by (1).

Equation (5) with (8) (and $W_{nmp} = 0$) gives the full inhomogeneity-capturing model for the dissipation tensor:

$$\epsilon_{ij}^{I} = 2\nu\bar{Q}_{im,p}\bar{Q}_{jm,p} + \tfrac{2}{3}\tilde{\epsilon}R_{ij}, \tag{9}$$

where $\bar{Q}_{ij}$ is taken to be the symmetric square root of the Reynolds stress tensor.

Note that when using the classical models, ϵ must be specified. The quantity ϵ equals the dissipation of mechanical energy only in homogeneous turbulence (for clarification

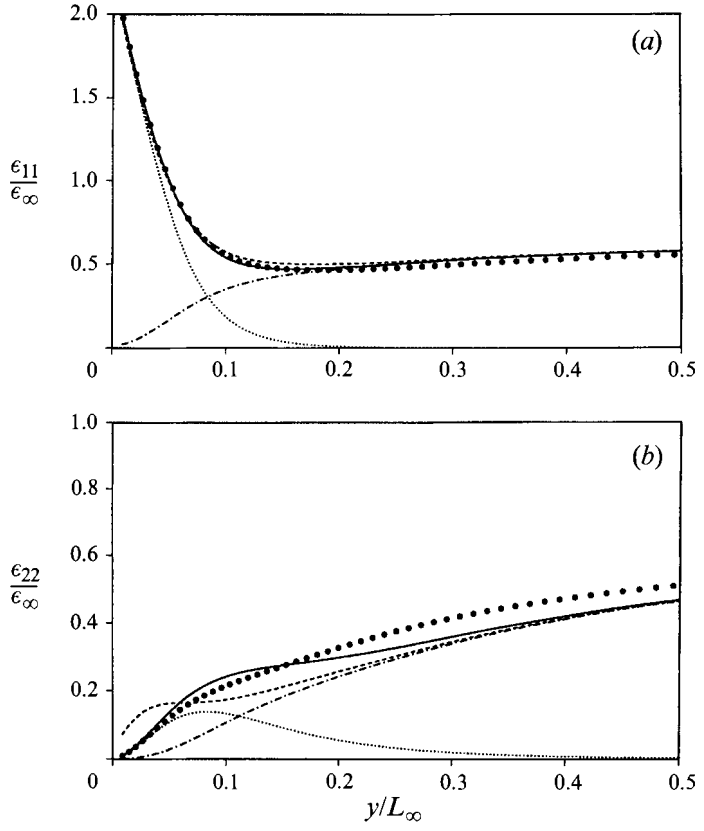

FIGURE 2. Dissipation near a shear-free solid wall ($Re_\tau = 134$, $t/T_\infty = 2.0$). (*a*) Tangential dissipation, (*b*) normal dissipation: ●, DNS data of Perot & Moin (1995); ----, Rotta model; ——, inhomogeneity model; ....., 1st term of (9); —·—, 2nd term of (9).

on this point, see Bradshaw & Perot 1993). Otherwise, it appears in the Reynolds stress transport equations principally as a scaling parameter. The quantity $\tilde{\epsilon}$ also acts as a scaling parameter: it is an inverse timescale. The magnitude of $\tilde{\epsilon}$ can be derived from ϵ (or vice versa) by requiring the trace of the inhomogeneity model to equal 2ϵ. In the tests of the models, these quantities will be supplied from direct numerical simulation data, but in an actual modelling situation, they would have to be derived in some other manner (usually from a dissipation transport equation). The inverse timesale, $\tilde{\epsilon}$, is smoother near walls than ϵ, and impacts the overall model less in the near-wall region, because the terms involving $\tilde{\epsilon}$ go to zero near the wall. This is an important point as it means that the near-wall behaviour of the model depends only on the Reynolds stresses, not on some model quantity such as ϵ or $\tilde{\epsilon}$.

Figure 2 shows the non-zero components of the dissipation tensor near a shear-free wall (Part 1). Both the Rotta model and the inhomogeneity model capture the tangential dissipation well (figure 2*a*). The breakdown of the inhomogeneity model into its two principal terms shows that the 'exact' inhomogeneous term dominates close to the wall. The normal dissipation (figure 2*b*) shows more variation between the models. Close to the wall the inhomogeneous term dominates, and is exact. The Rotta model goes to zero at the wall, but at the wrong rate. Away from the wall, the two models are very similar. This is by design, since the inhomogeneity model reverts to the Rotta model when inhomogeneity is not important.

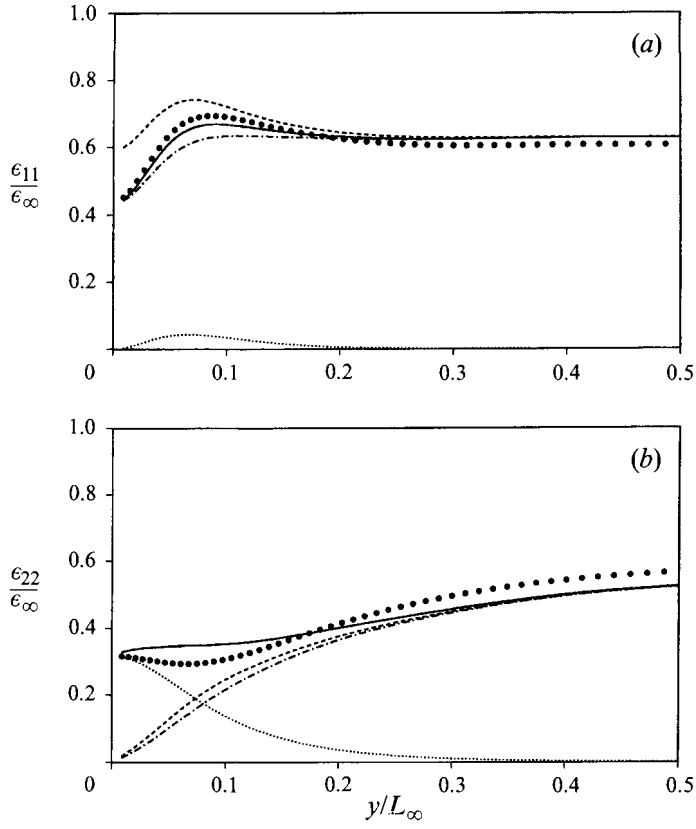

FIGURE 3. Dissipation near a free surface ($Re_T = 134$, $t/T_\infty - = 2.0$). (*a*) Tangential dissipation, (*b*) normal dissipation. See figure 2 for legend.

Note that given the right blending function, a mixed model of the type suggested by Hanjalic & Launder (1976) could also produce good results for this particular flow. However, this introduces a degree of empiricism not present in the current model. It is unlikely that a mixed model tuned for the solid wall would produce reasonable results for turbulence near a free surface.

The case of turbulence near a free surface (also described in Part 1) is shown in figures 3(*a*) and 3(*b*). Turbulence near a free surface is only mildly inhomogeneous. Nonetheless, the inhomogeneity model continues to perform well, and obtains the exact limiting value at the surface for both components of the dissipation. The Rotta model overpredicts the tangential dissipation near the surface, and severely underpredicts the normal dissipation. Note that a mixed model (with a blending function based solely on the Reynolds number) has little chance of success for this flow, since the turbulent Reynolds number is nearly constant across the domain, and neither the isotropic model nor the Rotta model captures the dissipation behaviour adequately over the entire domain.

The final test of the model is presented in figure 4(*a–d*). This shows the case of fully developed channel flow, where mean shear is an important factor. The data are from Mansour *et al.* (1988). Both the Rotta model and the inhomogeneity model work well for the streamwise component of the dissipation, though the inhomogeneity model captures the near-wall behaviour somewhat better. Far from the wall, the inhomogeneity model is only as good as the Rotta model (which, by design, it mimics

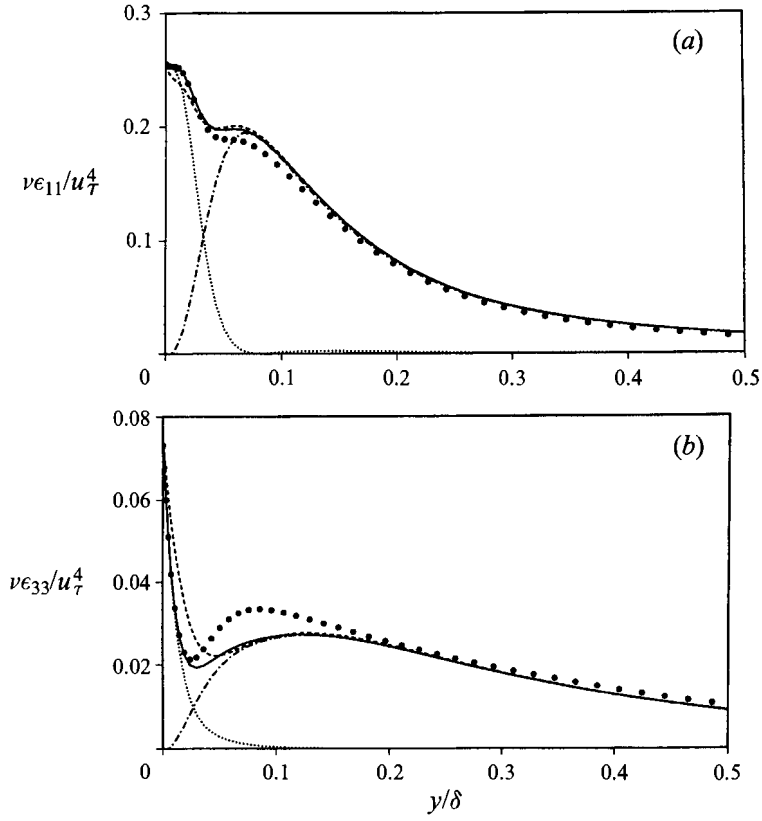

FIGURE 4(*a*, *b*). For caption see facing page.

when inhomogeneity is small). The spanwise component of the dissipation is very similar to the streamwise one. Again, both models perform well, with the inhomogeneity model capturing the near-wall behaviour almost exactly. The normal dissipation and off-diagonal dissipation, ϵ_{12}, also show very good near-wall behaviour when the inhomogeneity model is used. However, there is a significant underprediction of ϵ_{22} and overprediction of ϵ_{12} away from the wall. This is a result of the structure dissipation model. Improvements in these dissipation components will occur when better quasi-homogeneous dissipation models are developed. The Appendix suggests that improved quasi-homogeneous models might include terms involving Reynolds stress anisotropy. Although the model for the off-diagonal dissipation looks poor, it could produce very reasonable results when used in a full closure. This is because only the very near-wall dissipation is important in the evolution of R_{12}. Away from the wall, where the model agreement is not as good, the dissipation is not an important term (see Mansour *et al.* 1988). Tests of the model in an adverse pressure gradient boundary layer (Yang Na 1994, private communication) show very similar behaviour.

The inhomogeneity model extends classical quasi-homogeneous dissipation models into the very near-wall region. It gives extremely good agreement very close to a wall or boundary. However, away from the boundary, the inhomogeneity model is only as good as the quasi-homogeneous model upon which it is based. We have chosen to use the Rotta model in these demonstrations. If better quasi-homogeneous dissipation models exist, or are developed in the future, they can easy be incorporated into this framework.

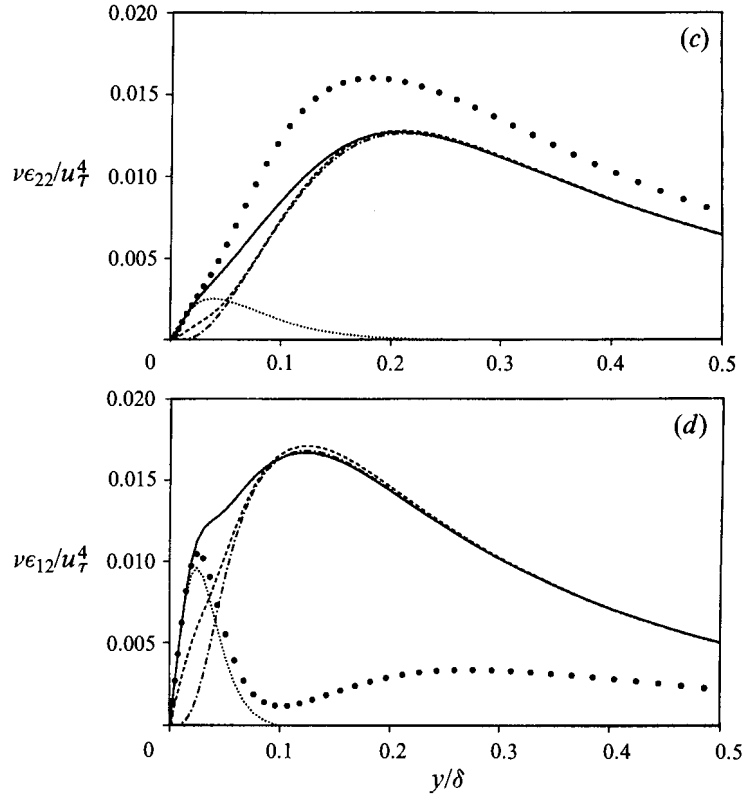

FIGURE 4. Dissipation in turbulent channel flow. (*a*) Streamwise dissipation, (*b*) spanwise dissipation, (*c*) normal dissipation, (*d*) shear stress dissipation. ●, DNS data of Mansour *et al.* (1988); – – –, Rotta model; ——, inhomogeneous model; ....., first term of (9); —·—, second term of (9).

3. Pressure–strain model

3.1. *Introduction*

The classic model for the (slow) pressure–strain term, is the Rotta (1951) return-to-isotropy model, $\Pi_{ij} = -c_1 \epsilon a_{ij}$, where $a_{ij} = R_{ij}/k - 2/3\delta_{ij}$. Return to isotropy has been shown to occur in homogeneous turbulence in the experiments of Lumley & Newman (1977). More recent models for the slow pressure–strain continue to be based on the idea that the pressure–strain must be a function of the Reynolds stress anisotropy tensor. These models add higher-order terms in the anisotropy tensor, a_{ij}, to the standard Rotta model. Examples of models of this type are Launder & Tselepidakis (1991), and Speziale, Sarkar & Gatski (1991).

The models of Lumley (1978) and Shih & Lumley (1986) take the slightly different approach of including the anistropy of the dissipation tensor into the return-to-isotropy model, so that $\Pi_{ij} - \epsilon_{ij} + (2/3)\epsilon\delta_{ij} = -\beta\epsilon a_{ij}$. This results from examination of the evolution equation for the anisotropy tensor in shear-free homogeneous turbulence,

$$a_{ij,t} = \frac{1}{k}(\Pi_{ij} - \epsilon_{ij} + \tfrac{2}{3}\epsilon\delta_{ij} + \epsilon a_{ij}). \tag{10}$$

In shear-free homogeneous turbulence, $\beta > 1$ guarantees return to isotropy, and $\beta = 1$ indicates no change in the anisotropy tensor with time (which Lumley suggests is the

high Reynolds number limit). At low Reynolds numbers, $\epsilon_{ij} - (2/3)\epsilon\delta_{ij} \to \epsilon a_{ij}$, and no return to isotropy is expected (see Lumley 1978), so $\Pi_{ij} \to 0$ (this phenomenon has been observed in the experiments of Hallback & Johansson 1992). Note that these previous conditions only strictly apply in shear-free homogeneous turbulence. For inhomogeneous turbulence, return to isotropy is neither expected, nor observed.

When boundaries are present, the slow pressure–strain term can be split into a standard nonlinear part, and a 'wall reflection part' because the usual free-space Green's function changes close to the boundary (Launder *et al.* 1975). Since both terms are 'slow' (do not depend explicitly on changes in the mean velocity gradients) we will model them collectively. However, we will show that the slow pressure–strain near a boundary is fundamentally different from the pressure–strain term occurring in quasi-homogeneous flows (far from the boundary), and the proposed model will take this change in behaviour into account.

3.2. *Pressure–strain model*

There have been various proposals on how to include near-wall effects into the pressure–strain term. Shih & Lumley (1986) include a coordinate dependence (L/y) into the coefficient β. Launder & Shima (1989) and Launder & Tselepidakis (1991) use the wall-normal vector and damping functions based on the wall-normal coordinate direction. In this work, we abandon such geometry-dependent formulations and attempt to produce a near-wall pressure–strain model based on the physical processes that occur near the wall (for a similar approach see Durbin 1993).

The physical insights into near-wall turbulent flow developed in Part 1 are a useful guide to this type of pressure–strain modelling. In Part 1 it was shown that the near-wall region can be viewed as a balance between two opposing events: impingements (splats) and ejections (antisplats). Both of these events transfer energy among the Reynolds stress components (the essence of the pressure–strain term), but they tend to exactly cancel unless viscous effects are present. So near boundaries viscous effects (dissipation and diffusion) tend to control the amount of intercomponent energy transfer. This is a considerably different process from that which occurs in homogeneous turbulence, where it is relatively clear that anisotropy in the Reynolds stresses causes intercomponent energy transfer. The different processes are reflected by the fact that in homogeneous turbulence there is a return to isotropy, while near boundaries there is a tendency to move away from isotropy.

Figure 5(*a*) shows DNS data for the pressure–strain term ($\Pi_{11} = -\frac{1}{2}\Pi_{22}$) near a shear-free solid wall at $Re_T = 134$ and time $t/T_0 = 1.0$. Close to the wall, there is a large transfer of energy from the normal stress component to the tangential stress components. This is due to the imbalance between splats and antisplats. A plot of the anisotropy in the dissipation and diffusion terms (also figure 5*a*) shows that there is very strong correlation between those terms and the peak in the pressure–strain close to the wall. We believe that this correlation exists because, close to the wall, viscous processes control the rate of intercomponent energy transfer.

Farther away from the wall the pressure–strain becomes negative, indicating a transfer of energy from the tangential stresses to the normal stress component. This is the more standard return-to-isotropy type of behaviour. The return-to-isotropy model $(-\epsilon a_{ij})$ is also plotted in figure 5(*a*). It shows very good agreement with the DNS data in the region far from the wall.

The following model for the pressure–strain is therefore proposed:

$$\Pi_{ij} = C_\pi e_{ij} - \beta\bar{e}a_{ij}, \tag{11}$$

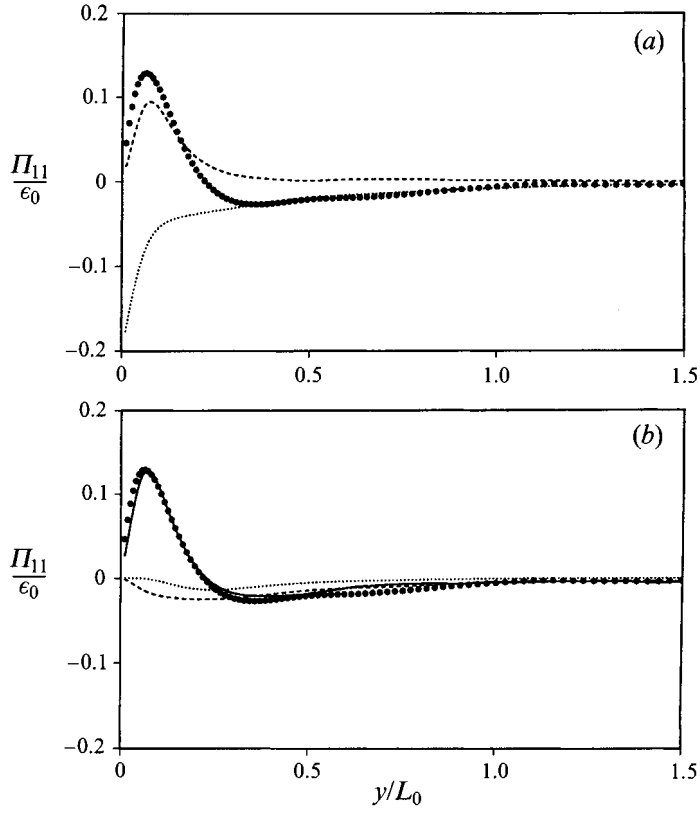

FIGURE 5. Pressure–strain near a shear-free wall ($Re_T = 134$, $t/T_0 = 1.0$): (*a*) ●, DNS data; ----, dissipation/diffusion anisotropy; ....., return-to-isotropy model. (*b*) ●, DNS data; ----, Lumley's model; ....., Launder & Tselepidakis' model; ——, present model.

where $e_{ij} = \epsilon_{ij} - \nu R_{ij,kk} - (2/3)\bar{e}\delta_{ij}$ is the dimensional anisotropy in the diffusion and dissipation tensors, and $\bar{e} = (\epsilon_{ii} - \nu R_{ii,kk})/2$ is the trace of these viscous tensors. For homogeneous flows, and $C_\pi = 1$, equation (11) is identical to the model of Lumley. For inhomogeneous flows, there are some important differences. This model includes anisotropy of the diffusion term along with anisotropy of the dissipation, and the return to isotropy has been modified by including the trace of the diffusion term. As indicated previously, we believe that the inclusion of dissipation plus diffusion is more appropriate for near-wall inhomogeneous flows than the dissipation alone. Using the trace of the dissipation and the diffusion in the return-to-isotropy term (rather than just ϵ) follows logically from this choice, and has the added benefit of causing the return-to-isotropy term to go to zero near the wall where the return-to-isotropy mechanism does not appear to play an important role (figure 5*a*).

The choice of $C_\pi = 1$ results in a Reynolds stress equation closure in which only the trace of the dissipation tensor needs to be modelled (not the tensor itself). Perhaps this was partly Lumley's motivation for this choice. However, the DNS data suggests $C_\pi \neq 1$. When $C_\pi \neq 1$ an accurate model for the dissipation tensor is required. The issue of accurate dissipation tensor modelling has been addressed in §2.

Using (11), the conditions on the return-to-isotropy coefficient β change slightly. In high Reynolds number homogeneous turbulence β still goes to a value of one. However, in low Reynolds number homogeneous turbulence $\beta \to C_\pi$ (rather than

$\beta \to 1$ as in the Lumley model). When the turbulence is inhomogeneous little can be said about these coefficients. In what follows the choice, $C_\pi = 2.3$ and $\beta = 1 + 1.3A \exp(-Re_T^{1/2})$ will be used, where A is the 'flatness' parameter described in §2.5, and Re_T is the turbulent Reynolds number. This choice for β is functionally very similar to that proposed by Lumley (1978). It produces the correct Reynolds number limits in homogeneous flow. The value for C_π was chosen to fit the simulation data. For the near-wall situations studied herein, either A is very small (near the wall) or $\exp(-Re_T^{1/2})$ is small (away from the wall), so $\beta \approx 1$ throughout these flows. This means that the model results presented herein essentially use the value $\beta = 1$; they do not test the general validity of the expression for β.

The use of dissipation anisotropy for a (slow) pressure–strain model is strongly reminiscent of the practice of using production anisotropy $(P_{ij} - P_{kk}\delta_{ij}/3)$ in fast pressure–strain models (Launder & Shima 1989). Energy source terms (like production) could easily affect turbulence in a similar way to viscous sink terms (dissipation and diffusion). We find it very appropriate to model the fast and slow terms of the pressure–strain in this complementary manner.

3.3. *Results*

A comparison of the present model (equation (11)) with DNS data, and other slow pressure–strain models is shown in figure 5(*b*) for turbulence near a shear-free solid wall. The present model, which includes the effects of dissipation and diffusion anisotropy, shows very good agreement with the DNS data.

The model of Lumley (1978) is essentially

$$\Pi_{ij} = \epsilon_{ij} - \tfrac{2}{3}\epsilon\delta_{ij} - \epsilon a_{ij}. \tag{12}$$

This assumes a value $\beta = 1.0$. Lumley gives a more complicated expression for β, but in these flows this complicated expression reduces to $\beta \approx 1.0$. Lumley's model is not designed for strongly inhomogeneous flows, so good agreement with the DNS data close to the wall is not expected. It is presented here because it is the starting point for the present model and shows the improvement resulting from these proposed modifications.

The model of Launder & Tselepidakis (1991) is specifically designed for near-wall flows. It is given by the expression

$$\Pi_{ij} = -c_1\,\epsilon(a_{ij} + 0.7(a_{ik}\,a_{kj} - a_{mn}\,a_{nm}\,\delta_{ij}/3)), \tag{13}$$

where

$$c_1 = 6.3A[\min(A, 0.6)]^{1/2}[1 - \max(1 - Re_T/140, 0.0)]. \tag{14}$$

This is essentially a nonlinear extension of the return-to-isotropy model. For this reason (and the fact that c_1 strongly damps the model near a boundary) this model does not capture the near-wall intercomponent energy transfer effects due to splats and antisplats.

Similar results for turbulence near a free surface (see Part 1) are shown in figure 6. As in the previous figure, the turbulent Reynolds number of the flow is initially 134, and the time at which the models were evaluated is $t/T_0 = 1.0$. Figure 6(*a*) shows DNS data for the pressure–strain, as well as the anisotropy in the dissipation and diffusion and the return-to-isotropy term $(-\epsilon a_{ij})$. The magnitude of the pressure–strain term near a free surface is generally smaller than that near a solid wall. However, many of the qualitative features remain similar. Close to the surface, the turbulence moves away from isotropy. The anisotropy of the combined dissipation and diffusion correlates fairly closely with this near-wall behaviour. Farther away from the wall, the more

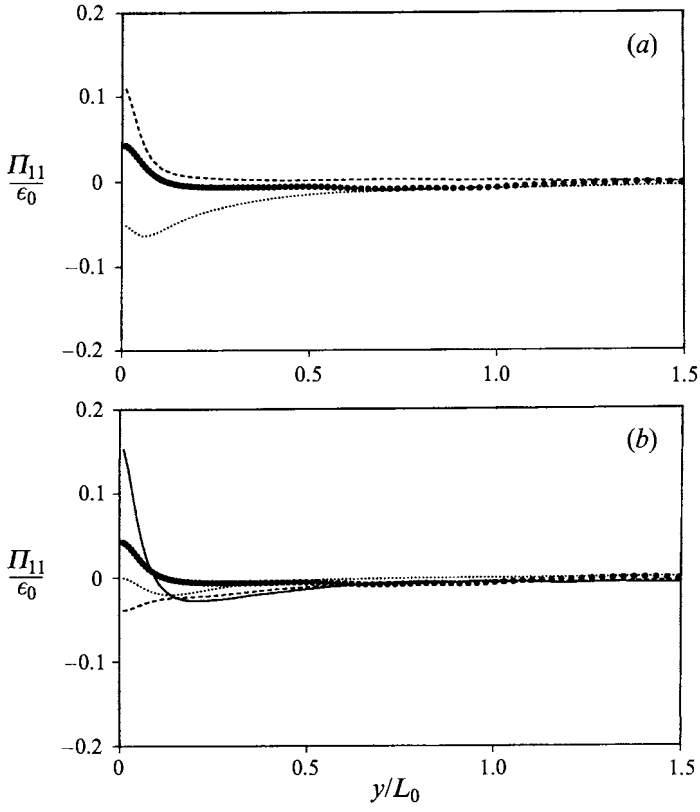

FIGURE 6. Pressure–strain near a free surface ($Re_T = 134$, $t/T_0 = 1.0$). See figure 5 for legend.

standard return-to-isotropy type of behaviour is recovered, and close agreement with the return-to-isotropy term is found.

Figure 6(*b*) indicates how the various models perform for turbulence near a free surface. The agreement of the present model with the DNS data is not good in this situation. However, the model does display the right qualitative features: return to isotropy far from the surface, and a sharp increase in the pressure–strain very close to the wall. A change in the value of C_π (to 0.5) gives a model that agrees very closely with the DNS data, and which outperforms the other two models. This indicates that C_π would be better represented as a function of the Reynolds stress invariants. Determination of this function is a subject of present research.

4. Conclusions

A new modelling technique for extending classical dissipation models into regions of large inhomogeneity has been developed. It is derived from a simple mathematical decomposition, and uses the square root of the Reynolds stress tensor as a generalized turbulent intensity to transform (or map) the fluctuating velocity into a quasi-homogeneous quantity (the velocity structure). The resulting inhomogeneity model, derived from this decomposition, satisfies all known mathematical constraints and is relatively simple to implement. It has been shown that the model gives superior results in both wall and surface bounded flows, as well as shearing flows. The mathematical formalism developed for the dissipation model has also been applied, with success to

the modelling of the scalar dissipation and heat flux dissipation (Malan & Johnston 1993).

The slow pressure–strain model presented herein generalizes the (quasi-homogeneous) model of Lumley, so that the model is appropriate near boundaries. The principal alterations were: (i) the use of dissipation and diffusion for both the leading anisotropy term and the scaling of the return to isotropy term, and (ii) a non-unity coefficient, C_π. It appears that C_π (like β) is best represented as a function of the various tensor invariants, but this functional dependence has not been explored further.

Financial support for this work was provided by the National Science Foundation and the Center for Turbulence Research. Supercomputer time on the Connection Machine was provided by the NAS Division of NASA-Ames Research Center. The authors would like to thank Mr Yang Na for his detailed examination of the dissipation model. Useful discussions with Dr Paul Durbin are appreciated.

Appendix. Dissipation tensor realizability

This Appendix examines some of the consequences of using the dissipation tensor model (proposed in §2) in a full Reynolds stress closure. In particular, we will focus on the low Reynolds number limit, where viscous effects (dissipation and diffusion) dominate. In this limit the Reynolds stress equations become

$$\boldsymbol{R}_{,t} = \nu \boldsymbol{R}_{,kk} - \boldsymbol{E}. \tag{A 1}$$

The ij tensor notation has been dropped in favour of a simpler matrix representation of the problem, where $\boldsymbol{R}$ is the Reynolds stress tensor, R_{ij}, and $\boldsymbol{E}$ is the dissipation tensor, ϵ_{ij}.

Using the identity $\boldsymbol{R} = \boldsymbol{Q}\boldsymbol{Q}^T$ and modelling the dissipation tensor with (5) and $W_{nmp} = 0$ gives

$$(\boldsymbol{Q}_{,t} - \nu \boldsymbol{Q}_{,kk})\,\boldsymbol{Q}^T + \boldsymbol{Q}(\boldsymbol{Q}_{,t}^T - \nu \boldsymbol{Q}_{,kk}^T) = -\boldsymbol{Q}\tilde{\boldsymbol{E}}\boldsymbol{Q}^T, \tag{A 2}$$

where $\tilde{\boldsymbol{E}}$ is the structure dissipation tensor, $\tilde{\epsilon}_{ij}$.

It is now assumed that $\tilde{\boldsymbol{E}}$ is modelled in terms of the Reynolds stress tensor. This means that we can write $\tilde{\boldsymbol{E}} = f(\boldsymbol{R})$, where f is some analytical function. All dissipation models known to the authors fall into this category. This assumption implies that $\tilde{\boldsymbol{E}}$ and $\boldsymbol{R}$ have the same eigenvectors (principal directions). If $\boldsymbol{Q}$ is taken to be the symmetric square root of $\boldsymbol{R}$, then $\boldsymbol{Q}$ also has the same principal directions as $\boldsymbol{R}$ and $\tilde{\boldsymbol{E}}$.

Writing (A 2) in the principal coordinate system gives

$$(\hat{\boldsymbol{Q}}_{,t} - \nu \hat{\boldsymbol{Q}}_{,kk})\,\hat{\boldsymbol{Q}}^T + \hat{\boldsymbol{Q}}(\hat{\boldsymbol{Q}}_{,t}^T - \nu \hat{\boldsymbol{Q}}_{,kk}^T) = -\hat{\boldsymbol{Q}}\hat{\boldsymbol{E}}\hat{\boldsymbol{Q}}^T, \tag{A 3}$$

where a hat indicates the quantity is evaluated in the principal system. $\hat{\boldsymbol{Q}}$ and $\hat{\boldsymbol{E}}$ are therefore diagonal matrices, $\hat{\boldsymbol{Q}}_{,t}$ and $\hat{\boldsymbol{Q}}_{,kk}$ need not be diagonal.

Note that if the diagonal components of $\hat{\boldsymbol{Q}}$ are non-zero, and $\boldsymbol{Q}$ is a symmetric tensor (which it is), then (A 3) implies that the off-diagonal components of $\hat{\boldsymbol{Q}}_{,t} - \nu \hat{\boldsymbol{Q}}_{,kk}$ are zero. This in turn, means that we can write

$$\hat{\boldsymbol{Q}}_{,t} = \nu \hat{\boldsymbol{Q}}_{,kk} - \hat{\boldsymbol{Q}}\hat{\boldsymbol{E}}/2, \tag{A 4}$$

which is the expression invoked in §2.4 when discussing realizability.

REFERENCES

BRADSHAW, P. & PEROT, J. B. 1993 A note on turbulent energy dissipation in the viscous wall region. *Phys. Fluids* A **5**, 3305–3306.

DRIEST, E. R. VAN 1956 On turbulent flow near a wall. *J. Aero. Sci.* **23**, 1007–1011.

DURBIN, P. A. 1993 A Reynolds stress model for near-wall turbulence. *J. Fluid Mech.* **249**, 465–498.

GIBSON, M. M. & RODI, W. 1989 Simulation of free surface effects on turbulence with a Reynolds stress model. *J. Hydraulic Res.* **27**, 233–244.

HALLBACK, M. 1993 Development of Reynolds stress closures of homogeneous turbulence through physical and numerical experiments. Doctoral thesis, Department of Mechanics, Royal Institute of Technology, Stockholm.

HALLBACK, M. & JOHANSSON, A. V. 1992 Modeling of pressure-strain in homogeneous turbulence. *Advances in Turbulence 4* (ed. F. T. M. Nieuwstadt). Springer.

HANJALIC, K. & LAUNDER, B. E. 1976 Contribution towards a Reynolds-stress closure for low-Reynolds-number turbulence. *J. Fluid Mech.* **74**, 593–610.

LAI, Y. G. & SO, R. M. C. 1990 On near-wall turbulent flow modelling. *J. Fluid Mech.* **221**, 641–673.

LAUNDER, B. E., REECE, G. J. & RODI, W. 1975 Progress in the development of a Reynolds-stress turbulence closure. *J. Fluid Mech.* **68**, 537–566.

LAUNDER, B. & REYNOLDS, W. C. 1983 Asymptotic near-wall stress dissipation rates in a turbulent flow. *Phys. Fluids* **26**, 1157–1158.

LAUNDER, B. & SHIMA, N. 1989 Second-moment closure for the near-wall sublayer: development and application. *AIAA J.* **27**, 1319–1325.

LAUNDER, B. & TSELEPIDAKIS, D. P. 1991 Contribution to the modelling of near-wall turbulence. *Turbulent Shear Flows 8, Munich, Germany* (ed. F. Durst *et al.*), pp. 81–96. Springer.

LUMLEY, J. L. 1978 Computational modeling of turbulent flows. In *Advances in Applied Mechanics* (ed. C.-S. Yih), vol. 18, pp. 123–176. Academic.

LUMLEY, J. L. & NEWMAN, G. R. 1977 The return to isotropy of homogeneous turbulence. *J. Fluid Mech.* **82**, 161–178.

MALAN, P. & JOHNSTON, J. P. 1993 Heat transfer in shear-free turbulent boundary layers. *Rep.* MD-64. Dept. of Mech. Engng, Stanford University.

MANSOUR, N., KIM, J. & MOIN, P. 1988 Reynolds-stress and dissipation budgets in a turbulent channel flow. *J. Fluid Mech.* **194**, 15–44.

PEROT, B. & MOIN, P. 1995 Shear-free turbulent boundary layers. Part 1. Physical insights into near-wall turbulence. *J. Fluid Mech.* **295**, 199–227.

ROTTA, J. 1951 Statistical Theory of inhomogeneous turbulence. Part I. *Z. Phys.* **129**, 257–572.

SCHUMANN, U. 1977 Realizability of Reynolds stress turbulence models. *Phys. Fluids* **20**, 721–725.

SHIH, T. H. & LUMLEY, J. L. 1986 Second-order modeling of near-wall turbulence. *Phys. Fluids* **29**, 971–975.

SPEZIALE, C. G., SARKAR, S. & GATSKI, T. B. 1991 Modeling the pressure-strain correlation of turbulence. *J. Fluid Mech.* **227**, 245–272.

TSELEPIDAKIS, D. P. 1991 Development and application of a new second-moment closure for turbulent flows near-walls. PhD thesis, Dept. of Mech. Engng, University of Manchester.